Algorithm Theoretical Basis Document (ATBD) for large-scale oil spill detection using EOS-04

June-2023

Space Applications Centre
Indian Space Research Organisation
Ahmedabad-380015

Algorithm Theoretical Basis Document (ATBD) for large-scale oil spill detection using EOS-04

1. Algorithm Specifications:

Version	Date	Prepared by	Description
1.1	15/06/2023	Ratheesh Ramakrishnan, GSD/PGSG/EPSA	Automatic segmentation of dark area and classification into oil spill along the northern Indian Ocean using EOS-04 MRS systematic coverages

2. Summary:

Marine oil spill are a cause of concern among both the scientific and management communities. Timely detection of marine oil spill and dissemination of the information is essential for effective response and containment efforts. Here we have developed an algorithm to segment out dark regions from EOS-04 SAR images and classify the detected dark regions as oil spill and look alike. Land masking is carried out over the systematic coverage of EOS-04 MRS data and adaptive threshold method is applied to detect dark regions within the marine region of the SAR images. The dark region in the SAR images are also caused due to look alike and a technique is developed to classify the detected dark regions to oil spill and look alike based on the physical and textural properties of the detected dark regions. Few assumptions were made while developing the algorithm; the biogenic slicks tend to form complex structures with multiple branches, while oil spill are mostly linear in shape; ratio of segment mean to background mean will be low for oil spill, while the homogeneity and mean border gradient is expected to be high for oil spill. Based on these assumptions, look up tables are made and ranking are given to each detected dark region. Oil spills are then classified based on the total rank and an advisory in form of text file is created where the locations in lat lon is given for each classified oil spill. Shapefile is also generated having point location information of the detected oil spill.

3. Introduction:

The brightness in a SAR image for ocean surface is due to the wind-generated short gravity-capillary waves. The wave lengths of these short gravity-capillary waves are at comparable to the microwave and satisfies the Bragg resonance model given as

$$\lambda_w = \frac{n\lambda_r}{2\sin\theta},\ n = 1,2,3 \ldots \qquad \ldots\ldots\ldots\ldots\ldots (1)$$

where λ_w is the wave length of Bragg-selected ocean surface waves, λ_r is the radar wavelength and θ is the incidence angle.

On the ocean surface, presence of these waves makes the ocean surface rough as perceived by the radar wavelength and hence even for a relatively calm ocean; the sea surface have considerable contribution of backscatter at the radar sensor. When the slick covers the surface, the wind has less effect and amplitude of the wave decreases. Moreover, the surface stress gradient due to the visco-elastic property of the oil film acts against the up and down wave motion, which results in dampening of the short gravity-capillary waves. As the slick dampens the short gravity-capillary waves, the dynamic roughness of the ocean are reduced. As a consequence, radar backscattering level gets reduced in the slick affected region and in the radar image the slick region appears as a dark patch with weak backscattering in comparison with the surroundings. The gravity-capillary waves can also be dampened under the presence of natural biogenic surfactants or natural films; reducing the backscatter and giving an impression as oil spill in the radar images. The reduction of backscatter in the radar images may also occur due to low surface winds, rain cells and at shear zones. In the context of SAR image interpretation, they are collectively known as lookalike of oil spill (Solberg et al, 2007, Topouzelis 2008)

Dark formation in the SAR images; hence can be either due to oil spill or its lookalikes. Detection of the dark spots in the radar image is considered as the fundamental step in oil spill detection systems using SAR images. Dark spot detection is followed by feature extraction. Features of the dark spot are grouped into three, 1) shape: representing the geometry and orientation of the slick, 2) contrast or homogeneity: referring to the spectral behaviour of the spill and the 3) contextual features. Classification techniques are developed to discriminate the dark region into oil spill or lookalike based on the characteristics of the features extracted from the dark spots on the radar images. Neural network, fuzzy logic and statistical classifiers are the common techniques used to classify the detected dark spot into oil spill or lookalike (Ratheesh and Majumdar, 2013).

3.1 EOS-04 instrument

EOS-04 (RISAT-1A) was launched on 14-02-2022 from SDSC-SHAR, Sriharikotta. EOS-04 is a C-band (5.4 GHz, ±37.5 MHz) Synthetic Aperture Radar (SAR) mission, which is a follow-on mission of RISAT-1. The satellite is a polar sun synchronous orbiting satellite with 6AM and 6 PM equatorial crossing time. Launched at an altitude of 524.8 km, with an inclination of 97.554°, EOS-04 has single, dual, full and hybrid circular polarimetric capability (SAC, 2022).

The different mode of operation are given in table 1.The MRS systematic mode have 160 km swath and attain global coverage in 257 orbits in 17 days.

The level-1 product is made available in both CEOS and GeoTIFF formats except for SCANSAR and HRS level-1 SLC, which are available in GeoTIFF only. The level-2 product in EOS-04 is the level-2A enhanced Geo-referenced product of RISAT-1, which is given in GeoTIFF format in UTM, Geographic (SAC, 2021).

Table 1. Mode of operation of EOS-04 and its specifications

	Mode	Polarization Available	Resolution (Azimuth x Slant Range)	Nominal Swath	Noise equivalent Sigma naught (NESZ) (worst case)
1	Coarse Resolution ScanSAR (CRS)	Single/Dual/ Circular	48m x 8m	223km	-17.5 dB
2	Medium Resolution ScanSAR (6 Beam MRS)	Single/Dual/ Circular	23m x 8m	115km	-17.5 dB
3	Medium Resolution ScanSAR (8 Beam MRS)	Single/Dual/ Circular	33m x 8m	150-160km	-17.5 dB
4	Fine Resolution Stripmap-2 (FRS-2):	Expt full-polarimetry	3m x 4m	20km	-19.2 dB
5	Fine Resolution Stripmap-1 (FRS-1)	Single/Dual/ Circular	3m x 2m	25km	-17.5 dB
6	High Resolution Spotlight (HRS)	Single/Dual/ Circular	1m x 2m	15km	-18 dB

4. Theoretical Background:

Remote sensing technology, in particular the SAR images have a major role in the detection of natural and anthropogenic oil slicks. The all-weather, day and night capability and high resolution imaging of ocean surface have made SAR imaging technique to be accepted in the monitoring of oil spill in the marine environment. The major disadvantage of SAR image in the use of detecting the oil spill is look alike, due to biogenic slicks, low wind regions, rain cells or shear zones. Detection of oil spills from SAR images lacks a common algorithm (Alpers et al, 2017). The widely adopted methodology is dark spot analysis (Gade and Alpers, 1999; Brekke and Solberg, 2005). As oil dampens the capillary waves, the oil spill appears as dark spots. The dark spots are detected and are classified to oil spills based on various parameters extracted from the dark spot region.

The methodology adopted varies right from the techniques used to detect dark segments, the type and numbers of features extracted, and the classification technique. A comprehensive review of the existing methods used in the detection of oil spill can be seen in Jafarzadeh et al., (2021).

Oil spill detection algorithm can be broadly sequenced as dark area segmentation, feature extraction and classification. The goal of segmentation is to segment out all possible oil spill candidates. Dark spot segmentation are usually carried out by thresholding methods, where the adaptive threshold algorithm is the commonly used technique (Ratheesh and Majumdar, 2013). Histogram based threshold estimation, use of Bayesian models based on curve evolution and geometric flow and edge detection methods are the other methods applied in SAR images to segment out the oil spill candidates (Karantzalos and Argialas, 2008; Frate et al, 2000, Solberg et al, 2007)

The polarimetric capability of SAR images are also used in oil spill detection (Prajapati et al, 2021; Song et al, 2018). Polarimetric analysis involves the estimation of the polarimetric properties of the SAR backscattered signals, such as intensity, phase difference and polarization coherence to differentiate oil spills from look alike. Machine learning techniques have gained recent prominence in oil spill detection from SAR images that involves training algorithm to learn the pattern and features associated with oil spills observed from SAR images. Supervised algorithms like Support Vector Machines (SVM), Random Forest, or Convolutional Neural Networks (CNN) are most common methods used to classify the detected dark spots to oil spills (Ronci et al., 2020).

5. Algorithm Development:

Figure 1 shows the flowchart of the algorithm used to detect oil spill in the marine environment. In SAR images, oil spill are observed as dark spots. As explained, the short-gravity capillary waves that forms backscatter in the SAR images are dampened due to the presence of oil slick. This result in reduced return backscatter signals in SAR images and the region appear as dark compared to the surroundings. The dark regions in ocean waters observed from SAR images also can be caused due to the presence of other look alike namely, low wind shear, biogenic slicks. The objective of the present algorithm is to segment out the dark regions observed in the oceanic region from HH image of MRS systematic coverage and classify the dark segment as oil spills and look alike.

Satellite data

Level 2-A Enhanced Geo-Referenced product of Medium Resolution ScanSAR (MRS) systematic coverage mode is used to detect oil spill. The MRS systematic mode have a nominal repetivity of 17 days with 160 km swath width and a global coverage in 257 orbits. Features in oceans are observed in like polarisation modes of SAR images. Here we have used HH polarisation mode of the MRS systematic coverage that is exercised regularly during the morning 6 AM descending pass. The level-2A product is provided in GEOTIFF format along with two auxiliary files for Layover masking and Local incidence angle.

Pre-processing

The reflective strength of the radar target are determined by radiometric calibration where sigma-naught backscattering coefficients are computed by utilising the local incidence angle information and product calibration constant given within the BAND_META.txt

$$\sigma^{\circ} = \frac{(DN^2 - N)\sin i}{k_{cal\_Beta0\_Linear}} \quad \text{……………. (2)}$$

DN is the digital number, i is the local incidence angle, N is the IMAGE_NOISE_BIAS available for HH polarisation in BAND_META.txt, $k_{cal\_Beta0\_Linear}$ is estimated as

$$k_{cal\_Beta0\_Linear} = 10^{\left(\frac{k_{cal\_Beta0\_DB}}{10}\right)} \quad \text{……………. (3)}$$

$k_{cal\_Beta0\_DB}$ is the product calibration constant in db provided in BAND_META.txt

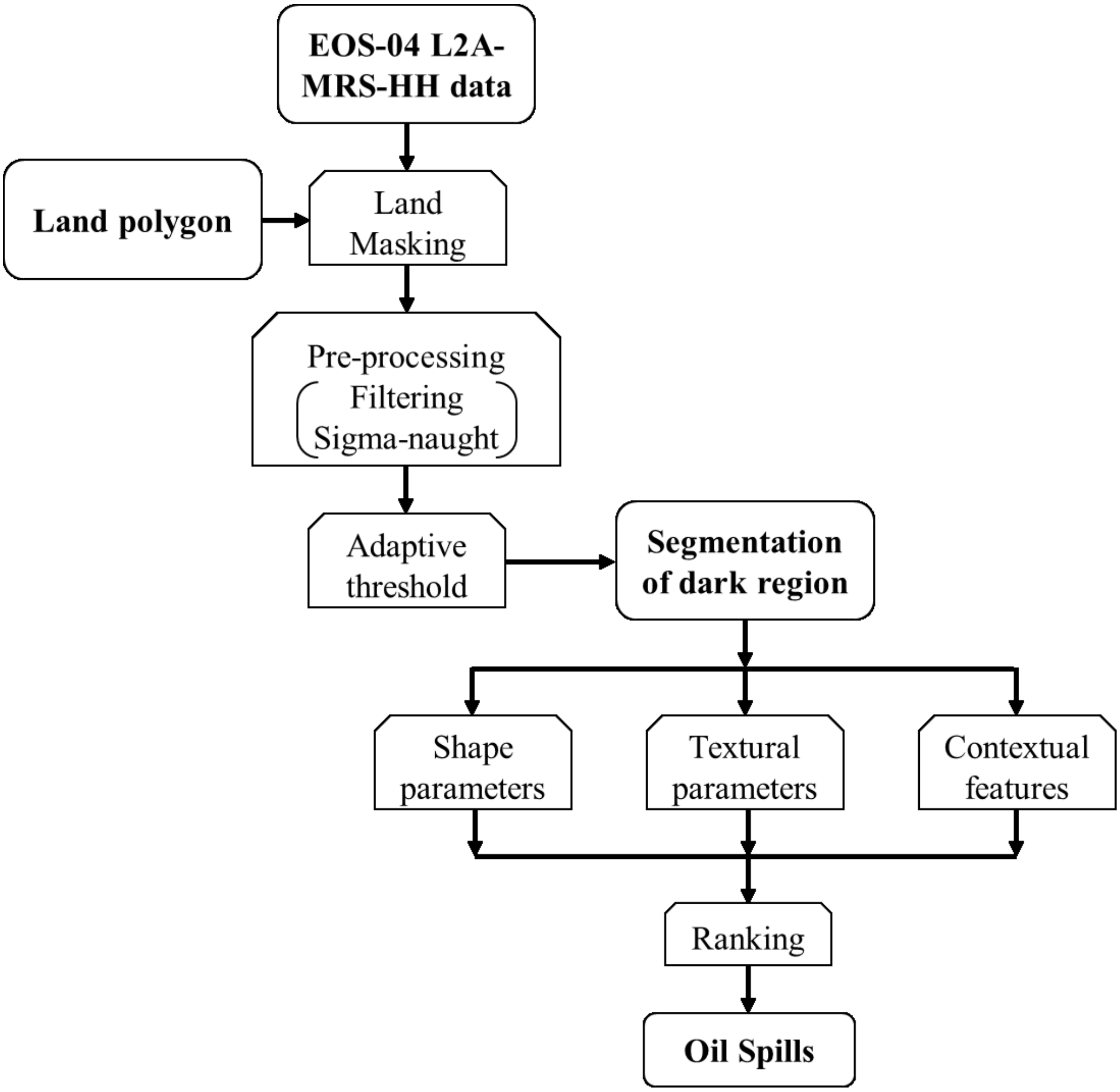

Figure 1. Flow chart of the oil spill detection algorithm

Speckles that results from the coherent interference of radar echoes from target produces salt and pepper appearance that degrades the SAR image, which reduces the seperability between oil spill region and the background (Xu et al. 2015; Wang, Zhang, and Patel 2017; Chierchia et al. 2017). Speckles are removed by applying Lee filtering technique (Lee et al, 1994).

Land masking

Oil spill detection is carried out for the ocean region of the Northern Indian Ocean. We have used Land polygon in geographic co-ordinates of the land mass covering the Northern Indian Ocean that includes Lakshadweep, Andaman and Nicobar Islands and the island of Sri Lanka (Figure 2). Mask is built for each individual L2A-MRS-HH scenes based on the corner coordinates thus avoiding pre-defined mask of larger size.

Information of corner coordinates are extracted for the input SAR image and the shapefile (Land polygon) is then clipped based on the corner coordinates. Care is taken to close the polygons that represents islands. The clipped polygon is then converted to raster with same size of the input SAR image, where value '1' is given for the ocean part.

Ship Detection

Ships/Rigs forms contextual parameter for the oil spill detection algorithm. The proximity of ship or oil rigs to the dark region increases the chance for the dark segment to be oil spill. The ship or the rigs acts as point target in SAR images with high backscatter values that can substantially alter the statistical parameters, hence they are to masked prior to the estimation of statistical parameters. Ship detection algorithm is formulated based on Constant False Alarm Rate (CFAR), where an improved CFAR algorithm based on Rayleigh distribution is performed (Wu 2021). CFAR is a pixel-level target detection algorithm where the targets have generally a strong contrast to the background clutter.

Probability of False Alarm

$$PFA = \int_T^{\infty} f_{pdf}(x)dx \quad \ldots\ldots\ldots\ldots\ldots(4)$$

where x is the grey value of the pixel and T is the detected threshold. When $x > T$, the pixel is considered as target.

The probability density function is given by Rayleigh distribution, where

$$f_{pdf}(x) = \frac{x}{\sigma^2} e^{-x^2/2\sigma^2}, x \geq 0 \ldots\ldots\ldots\ldots\ldots(5)$$

where σ is the distribution parameter, calculated using the Rayleigh distribution formula

$$\sigma = \frac{2\mu^2}{x} \quad \ldots\ldots\ldots\ldots\ldots(6)$$

where μ is the mean.

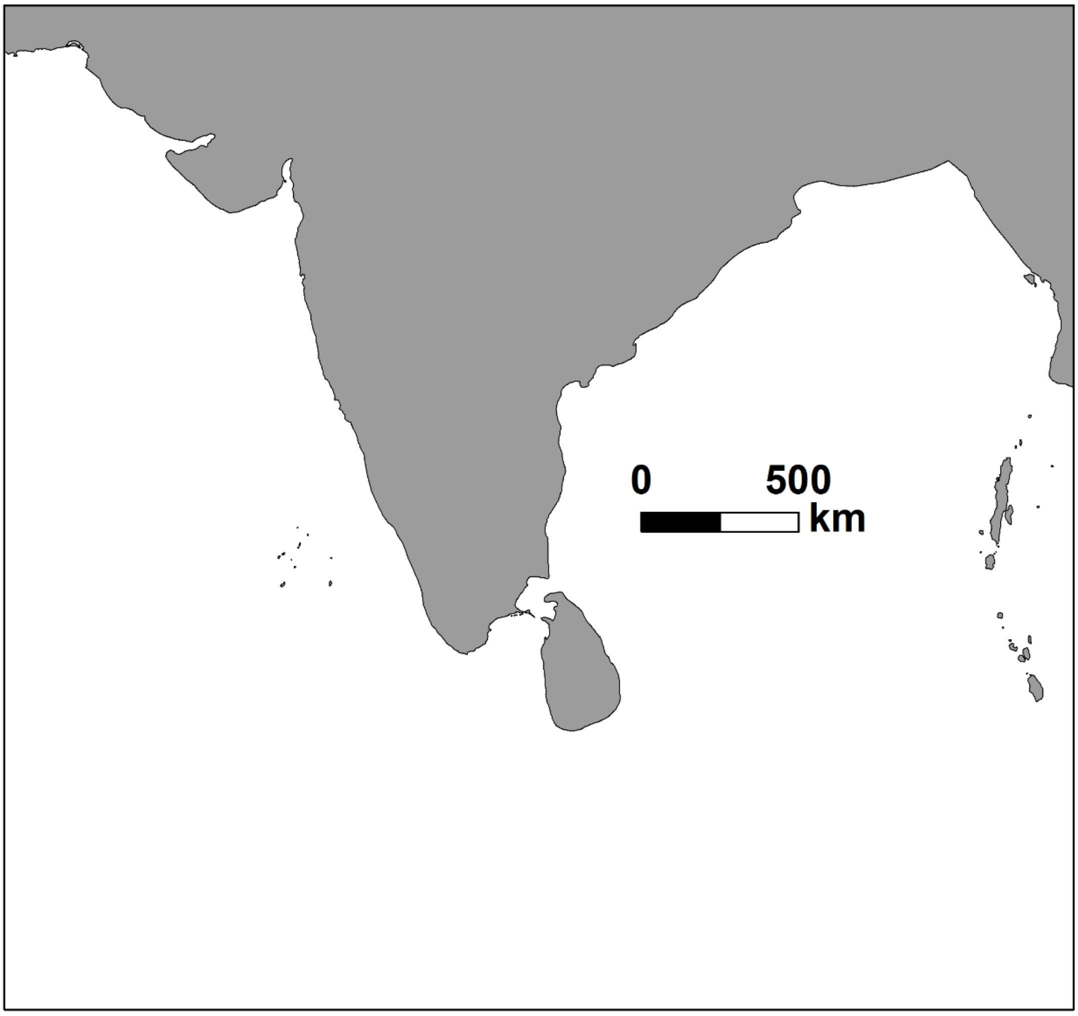

Figure 2. The Land polygon used to mask the landmass for oil spill detection algorithm

Segmentation of dark region

The adaptive threshold method proposed by Bradley and Roth (2007) is used, which is based on integral images. The integral image is computed by storing at each location $I(x, y)$ the sum of all values to the left and above of the pixel (x, y). The integral image is computed as

$$I(x, y) = \sum_{x' \leq x, y' \leq y} i(x', y') \text{................(7)}$$

By using the integral image, average of an s by s window of pixels centred at each pixel is computed. If the value of current pixel is t percentage, less than the average then the pixel is considered as dark segment. t is the threshold computed as the ratio of its intensity to the average of neighbouring pixels. The segmentation algorithm is applied that gives a binary image that segment out the dark regions.

Several morphological operations are carried out to smoothen the detected region. Region with a minimum connected pixel elements (15000) are only retained to remove small patches of dark segments. Background values detected within a dark segment are removed to ensure continuity. Dilation and blurring is carried out to smooth the edges of the detected dark segment.

Feature extraction

Features representing, shape and textural properties are extracted for each individual detected dark segments. Area (A) and perimeter (P) of the detected dark segments are computed. The complexity of the dark segment is computed as

$$C = \frac{A}{P} \text{...............(8)}$$

The length of major (Lma) and minor axis (Lmi) of the ellipse representing the detected dark segment are computed and roundness of the dark segment is estimated as

$$Ro = \frac{Lma}{Lmi} \text{...............(9)}$$

Mean (Md) and standard deviation of the sigma-naught value of the detected dark segments are estimated. Mean (Mb) and standard deviation of the background is estimated, where background pixel values are taken within a box created along the outer four coordinate of the detected dark segment. Ratio of the means of dark segment and the background is estimated as mean of the ratio (Rm)

$$Rm = \frac{Md}{Mb} \text{...............(10)}$$

Homogeneity (Hm) within the detected dark segments are estimated based on Grey Level Co-occurrence Matrix. Sobel gradient operator is applied to estimate the border gradient and mean of the border gradient is computed (Bm).

Classification of Dark segment into oil spill

Classification of the detected dark segment to oil spill is carried out based on ranking method. Ranking are made based on Berkke and Solberg (2005) and assumptions that are stated below.

Complexity (Area/Perimeter)(C)

Biogenic slicks tend to form complex structures with multiple branches, while oil spill form linear patches. Complexity will be small for oil spills, while complexity of biogenic slicks are larger.

Roundness (Major axis/Minor axis)(Ro)

Oil spill are mostly linear in shape, hence the roundness will be towards value 1 for look alike

Ratio of Segment mean to Background mean (Rm)

Low ratio of mean are expected for oil spill with more contrast is expected for oil spill between the dark segment and background

Homogeneity (GLCM) (Hm)
Homogeneity is expected to be high for oil spill, whereas the look alike, especially due to low wind shear and rain cells tend to show large variations of sigma-naught values within the affected region.

Mean of Border Gradient (Bm)
Due to the expected larger contrast of oil spill region with the background, the mean border gradient is expected to be high for oil spill.

Ship/Rigs in the vicinity
Oil spill are expected to have ship/rigs in their vicinity

Ranks are assigned to each detected dark segment based on the values of each parameters as shown in table 2

Table 2. Look up table to assign ranks based on the estimated parameter for each detected dark segments.

Rank	**1**	**2**	**3**	**4**	**5**
Complexity	500	400	300	200	100
Roundness	1	4	6	8	10
Ratio of Means	0.6	0.5	0.4	0.3	0.2
Homogeneity	0.3	0.4	0.5	0.6	0.7
Mean Border Gradient	0.001	0.002	0.005	0.008	0.01
Ship/Rig	No	-	-	-	Yes

Total rank of each dark segment is computed by adding the individual ranks of each parameters. The possibility of the dark segment to be oil spill is then estimated based on the total rank given in table 3.

Table 3. Categorisation based on total rank

Low	**Medium**	**Medium-High**	**High**
5-8	9-13	14-20	21-30

The detected dark segments are assigned as "unconfirmed oil spill" when the total rank falls within medium-high and high category.
The program gives advisory as text file giving the locations of detected oil spill and location of the oil spill marked over the HH image in jpeg format.

Analysis

The oil spill detection program has been analysed over set of MRS-HH Level 2A product of EOS-04. Figure 3 shows MRS-HH data of 12-April 2022. The segmented image using the adaptive threshold method is shown in figure 4.

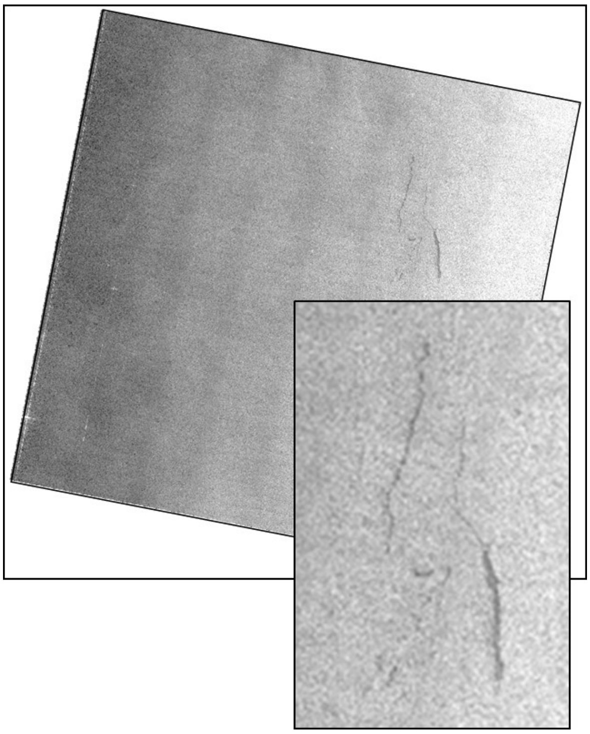

Figure 3. EOS-04 MRS-HH level 2A data set of 12-April-2022

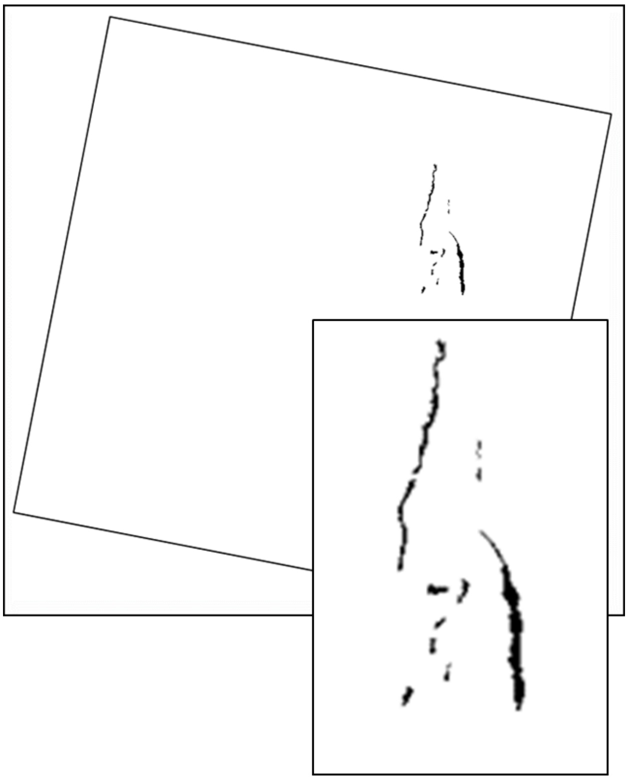

Figure 4. The segmented dark regions using adaptive threshold method

Based on the ranking system 4 oil spill regions are detected. Figure 5 shows the output jpeg image showing the location of unconfirmed oil spills for 12-April-2022 and table 4 shows the advisory of the detected oil spills and its location.

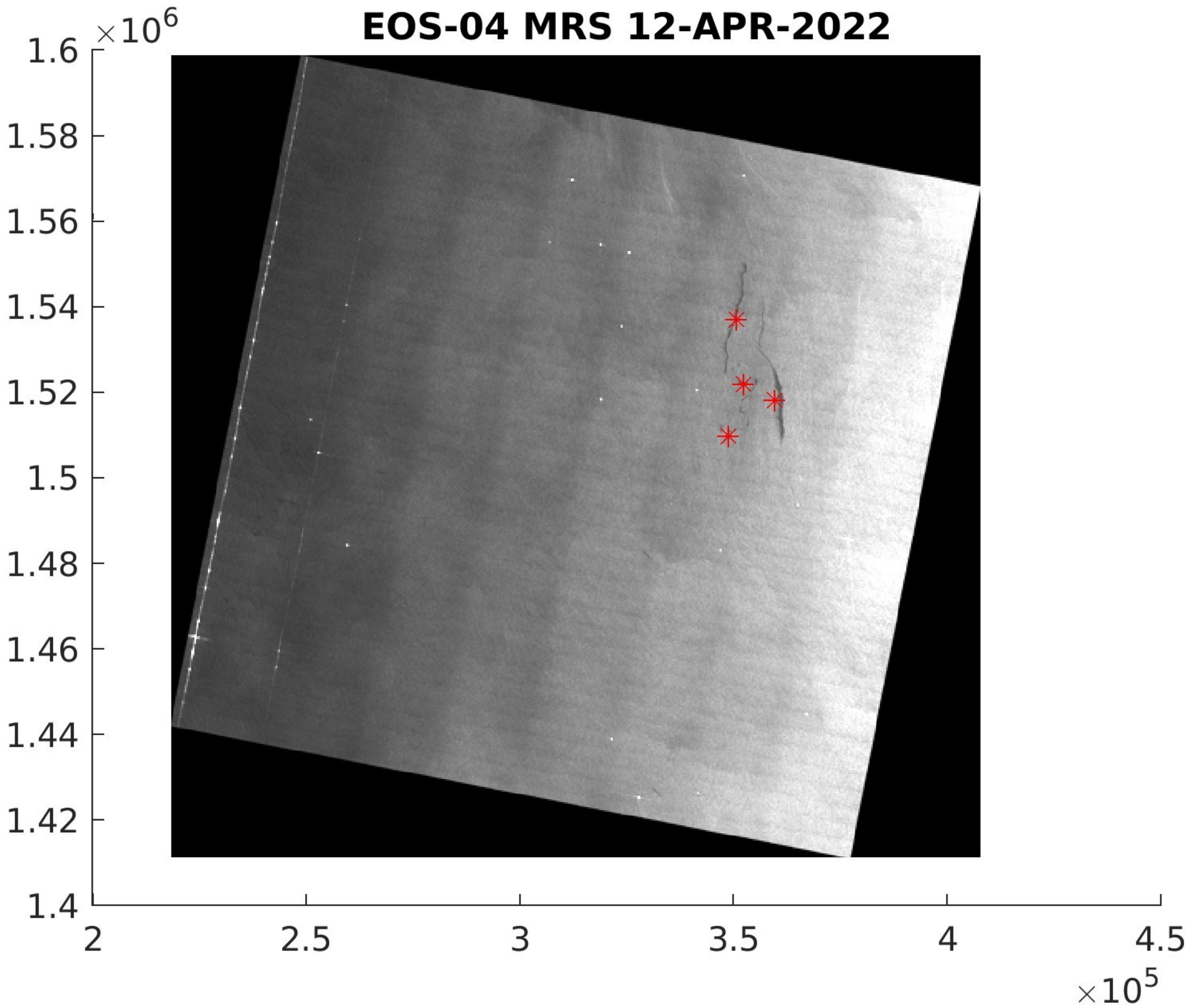

Figure 5. The detected oil spills marked over the SAR image

Table 4. Oil spill advisory

12-Apr-2022	
Unconfirmed oil spill with Medium-High Confidence at	
73.62	13.9
Unconfirmed oil spill with Medium-High Confidence at	
73.6	13.65
Unconfirmed oil spill with Medium-High Confidence at	
73.63	13.76
Unconfirmed oil spill with Medium-High Confidence at	
73.7	13.73

References

Alpers W.,Holt B and Zeng H. (2017). Oil spill detection by imaging radars: Challenges and pitfalls. Remote Sensing of Environment. 133-147.

Brekke C and Solberg A. (2005). Oil spill detection by satellite remote sensing, Remote sensing of environment. 95(1): 1-13.

Frate F.D. Petrocchi A. Lichtenegger J and Calabresi G. (2000). Neural networks for oil spill detection using ERS-SAR data, IEEE transactions on geosciences and remote sensing. 38(5): 2282-2287.

Gade, M., and W. Alpers. 1999. Using ERS-2 SAR for routine observation of marine pollution in European coastal waters. Sci. Total Environ. 237:38441–38448.

Jafarzadeh, H, Mahdianpari M, Homayouni S, Mohammadimanesh F and Dabboor M. (2021). Oil spill detection from Synthetic Aperture Radar Earth observations: A meta-analysis and comprehensive review. GIScience and Remote Sensing. 58(7): 1022-1051.

Karantzalos K and Argialas D. (2008). Automatic detection and tracking of oil spills in SAR imagery with level set segmentation. International journal of remote sensing. 26(6): 1157-1174

Prajapti K, R Ratheesh, B Madhuri, M Alka, N Zunnun, B Archana, et el (2022). Log Transformed Coherency Matrix for Differentiating Scattering Behaviour of Oil Spill Emulsions Using SAR Images. Mathematics 10 (10), 1697

Ratheesh R. and Majumdar T.J. (2013). Classification of oil spill in the Krishna-Godavari offshore using ERS-1 SAR images with a fuzzy logic approach, Indian Journal of Geo-Marine Sciences. 42(4), 431-436

Ronci, F. Avolio C. Donna M.D. Zavagli M. Piccialli V and Costantini M. (2020). Oil spill detection from SAR images by deep learning. IGARSS 2020 - 2020 IEEE International Geoscience and Remote Sensing Symposium

SAC, (2021) EOS-04 Data Products Formats (June 2022)-Version1.2, SAC/SIPG/MDPD/EOS-04/SAR/DP/2021/TN-05/Sep, 2021

SAC, (2022). RISAT-1A SAR: APPLICATIONS AND SCIENCE PLAN (Mar-2022)

Solberg A, Brekke C and Husoy P.O. (2007), Oil spill detection in RADARSAT and ENVISAT SAR images, IEEE Tans. Geosci and Rem. Sens. 45(3): 746-755

Song S. Zhao C. An W. Li X. and Wang C. (2018). Analysis of impacting factors on polarimetric SAR oil spill detection. Acta Oceanol. Sin. 37(11): 77-87

Topouzelis K. (2008). Oil spill detection by SAR images: dark formation detection, feature extraction and classification algorithms, Sensors, 8: 6642-6659